

The Dynamics of Supernumerary Tooth Development Are Differentially Regulated by Sprouty Genes



SVATAVA LAGRANOVA-CHURAVA^{1,2*},
FRANTISEK SPOUTIL¹,
SIMONA VOJTECHOVA¹, HERVE LESOT³,
MIROSLAV PETERKA¹, OPHIR D. KLEIN⁴,
AND RENATA PETERKOVA¹

¹Department of Teratology, Institute of Experimental Medicine AS CR, Prague, Czech Republic

²Department of Anthropology and Human Genetics, Faculty of Science, Charles University, Prague, Czech Republic

³INSERM UMR 1109, Team "Osteoarticular and Dental Regenerative NanoMedicine", and Dental School, Université de Strasbourg, Strasbourg, France

⁴Departments of Orofacial Sciences and Pediatrics and Program in Craniofacial and Mesenchymal Biology, University of California San Francisco, San Francisco, California

ABSTRACT

In mice, a toothless diastema separates the single incisor from the three molars in each dental quadrant. In the prospective diastema of the embryo, small rudimentary buds are found that are presumed to be rudiments of suppressed teeth. A supernumerary tooth occurs in the diastema of adult mice carrying mutations in either *Spry2* or *Spry4*. In the case of *Spry2* mutants, the origin of the supernumerary tooth involves the revitalization of a rudimentary tooth bud (called R2), whereas its origin in the *Spry4* mutants is not known. In addition to R2, another rudimentary primordium (called MS) arises more anteriorly in the prospective diastema. We investigated the participation of both rudiments (MS and R2) in supernumerary tooth development in *Spry2* and *Spry4* mutants by comparing morphogenesis, proliferation, apoptosis, size and *Shh* expression in the dental epithelium of MS and R2 rudiments. Increased proliferation and decreased apoptosis were found in MS and R2 at embryonic day (ED) 12.5 and 13.5 in *Spry2*^{-/-} embryos. Apoptosis was also decreased in both rudiments in *Spry4*^{-/-} embryos, but the proliferation was lower (similar to WT mice), and supernumerary tooth development was accelerated, exhibiting a cap stage by ED13.5. Compared to *Spry2*^{-/-} mice, a high number of *Spry4*^{-/-} supernumerary tooth primordia degenerated after ED13.5, resulting in a low percentage of supernumerary teeth in adults. We propose that Sprouty genes were implicated during evolution in reduction of the cheek teeth in Muridae, and their deletion can reveal ancestral stages of murine dental evolution. *J. Exp. Zool. (Mol. Dev. Evol.)* 320B: 307–320, 2013. © 2013 Wiley Periodicals, Inc.

J. Exp. Zool.
(*Mol. Dev. Evol.*)
320B:307–320,
2013

How to cite this article: Churava S, Spoutil F, Vojtechova S, Lesot H, Peterka M, Klein OD, Peterkova R. 2013. The dynamics of supernumerary tooth development are differentially regulated by Sprouty genes. *J. Exp. Zool. (Mol. Dev. Evol.)* 320B:307–320.

The adult mouse dentition is comprised of one incisor and three molars separated by a toothless gap (diastema) in each jaw quadrant. However, tooth primordia form in the diastema region during early development, and these will later stop developing, largely because of epithelial apoptosis. The presence of rudimentary tooth primordia in mouse embryos points to a relationship between the more complete dental pattern of evolutionary ancestors and the reduced pattern of extant mice (Peterkova et al., 2002, 2006; Prochazka et al., 2010). Two large rudiments, situated in the posterior part of the diastema and in front of the molar region, have been correlated with premolars lost during evolution (Peterkova et al., '96, 2000, 2002). The first experimental evidence of the existence of the two large rudiments called MS and R2 in the mouse mandible, as well as of their distinct signaling centers, sequential development and fate in wild-type (WT) mice, have been recently obtained using Dil labeling and markers of the signaling centers (Prochazka et al., 2010).

Interestingly, a supernumerary tooth is present in front of molars in several mouse mutants (Gruneberg, '55; Caton and Tucker, 2009; Cobourne and Sharpe, 2010; Wang and Fan, 2011). These supernumerary teeth have been interpreted as atavistic premolars that originate from the rudimentary anlage of the dentition in the diastema (Peterkova, '83; Peterkova et al., 2002, 2005; Ohazama et al., 2008, 2009; Pomtaveetus et al., 2011a,b). A supernumerary tooth also develops in Sprouty (*Spry*) null mice. In both *Spry2* and *Spry4* mutants, a supernumerary tooth occurs in front of the first molar (M1), and its frequency is much higher in the *Spry2*^{-/-} than in *Spry4*^{-/-} animals (Klein et al., 2006). However, the reason for this difference is not known.

Sprouty genes encode antagonists of Fgf signaling (Hacohen et al., '98), and they have been proposed to prevent rudimentary diastema buds from receiving sufficiently high levels of the Fgf signaling that normally sustains tooth development (Klein et al., 2006). Fgfs play a key role in early tooth development (Neubuser et al., '97; Peters and Balling, '99). The members of the Fgf family regulate important cellular activities. For example, *Fgf4* stimulates proliferation (Jernvall et al., '94; Vaahtokari et al., '96a) and prevents apoptosis (Vaahtokari et al., '96b) during tooth development. Increased *Fgf* signaling in *Spry2*^{-/-} mice has been proposed to explain the significantly increased proliferation and

decreased apoptosis in the R2 rudiment, which leads to its revitalization and development of the supernumerary tooth (Peterkova et al., 2009).

Whereas involvement of the R2 rudiment has been described in supernumerary tooth development in *Spry2* mutants, similar data about the *Spry4*^{-/-} embryos are missing, and in addition a potential role of the MS rudiment has not been investigated yet. Moreover, there is not yet a consensus regarding the impact of forming a supernumerary tooth on the size and morphology of the adult M1 in mutant mice (Gruneberg, '55; Sofaer, '69; Peterkova, '83; Kangas et al., 2004; Kassai et al., 2005; Klein et al., 2006; Ohazama et al., 2008, 2009). Therefore, we performed a prenatal and postnatal morphological and morphometric study, as well as 3D reconstructions combined with prenatal detection of expression domains of a marker of tooth signaling centers (sonic hedgehog—*Shh*), in *Spry2*^{-/-} and *Spry4*^{-/-} mice. We aimed first to compare the various developmental aspects of both rudimentary tooth primordia MS and R2 in the *Spry2*^{-/-} and *Spry4*^{-/-} mice and in WT mice, and second to determine and compare the role of MS and R2 in supernumerary tooth formation in mutants. We also tried to explain the consequences of such revitalization on the size and morphology of the M1 tooth in adult mice.

MATERIALS AND METHODS

Mice

Mouse lines carrying mutant alleles of *Spry2* (Shim et al., 2005) and *Spry4* (Klein et al., 2006) were maintained and genotyped as reported. The CD1 mice were purchased from Charles River (Sulzfeld, Germany) and were used as WT controls.

Mice and Embryos Harvesting and Staging

For prenatal studies, females were mated overnight, and noon after the morning detection of the vaginal plug was considered as embryonic day (ED) 0.5. The pregnant females were sacrificed by cervical dislocation at noon on ED12.5–15.5. For *Shh* expression, the pregnant mice were additionally sacrificed at 7–8 AM (corresponding to ED12.3, 13.3, 14.3) or 3–4 PM (corresponding to ED12.7, 13.7, 14.7) (Prochazka et al., 2010). These harvesting conditions enabled collection of a broader spectrum of developmental stages of the mouse embryos during the period under observation.

Immediately after taking the embryo or fetus out of the uterus, its wet body weight was determined after removing the excess of amniotic fluid on embryo surface by gentle dabbing on a dry Petri dish (till ED14.5) or on a filter paper (after ED14.5). The body weight allowed us to refine chronological staging of mouse embryos and to create a longitudinal series presenting subtle successive stages of tooth development (Peterka et al., 2002).

For postnatal study, adults of both sexes were sacrificed by cervical dislocation and their heads were fixed and kept in 70%

Grant sponsor: Grant Agency of the Czech Republic; grant number: CZ:GA ĆR:GAP305/12/1766.

*Correspondence to: Svatava Churava, Department of Teratology, Institute of Experimental Medicine, Academy of Sciences of the Czech Republic, v. v. i., Videnska 1083, 14220 Prague, Czech Republic.
E-mail: churava@biomed.cas.cz

Received 24 October 2012; Revised 28 February 2013; Accepted 1 March 2013

DOI: 10.1002/jez.b.22502

Published online 19 April 2013 in Wiley Online Library (wileyonlinelibrary.com).

ethanol for morphological and morphometric evaluation of adult teeth.

All of the animals' treatment satisfied the requirements of the Institutional Review Board of the Institute of Experimental Medicine, Academy of Sciences of the Czech Republic, Prague, Czech Republic.

Histology

The heads of embryos fixed in Bouin fluid or 4% PFA were routinely embedded in paraffin and cut in series of 7 µm thin frontal sections colored with alcian blue–hematoxylin–eosin or nuclear fast red.

3D Reconstructions

Drawings of the dental epithelium were traced from serial sections using a Leica DMLB microscope (Leica Microsystems GmbH, Wetzlar, Germany) equipped with a drawing chamber at a magnification of 320×. The drawings were memorized to computer (Lesot et al., '96) and the 3D reconstructions were created by VG-studio Max 2.0 software (VG-studio Max, Heidelberg, Germany). In some specimens, the *Shh* expression area was also recorded in the drawings and represented in the 3D reconstruction models.

Prenatal Quantitative Evaluation of Dental Epithelium on Histological Sections

A group of embryos exhibiting similar age and body weight was used for morphometric analysis of dental epithelium in each of three different mouse genotypes (WT, *Spry2*^{-/-}, *Spry4*^{-/-} mice) at ED12.5 and ED13.5. Each group comprised five left and five right mandible halves. In a mandible half, we evaluated consecutive serial sections in a representative region of tooth primordia MS, R2, and M1 (Fig. 1C,D). The rudiments MS and R2 were determined according to the typical shape of dental epithelium (Fig. 1A,B). The R2 rudiment could also be identified in the small supernumerary cap present in *Spry4*^{-/-} embryos at ED13.5 (compare to Fig. 4). The length of an evaluated region was identical in all jaws at a specific stage, but exhibited a difference between ED12.5 and 13.5 in accordance with the changing size of the tooth primordium (Fig. 1). Each evaluated section was photographed (magnification 500×) using a Leica DMLB microscope (Leica Microsystems GmbH) equipped with a camera Leica DC480 (Leica Microsystems GmbH).

The area of dental epithelium was measured and cells counted on each photographed section by software Image J (<http://rsbweb.nih.gov/ij>). The evaluated dental epithelium was delimited by the basement membrane, the oral surface of the epithelium, and the places where the thickness of the dental epithelium decreased to the thickness of the medially and laterally adjacent oral epithelium. The size of MS, R2, or M1 primordium was characterized by the average size of the dental epithelium on one section in the evaluated region.

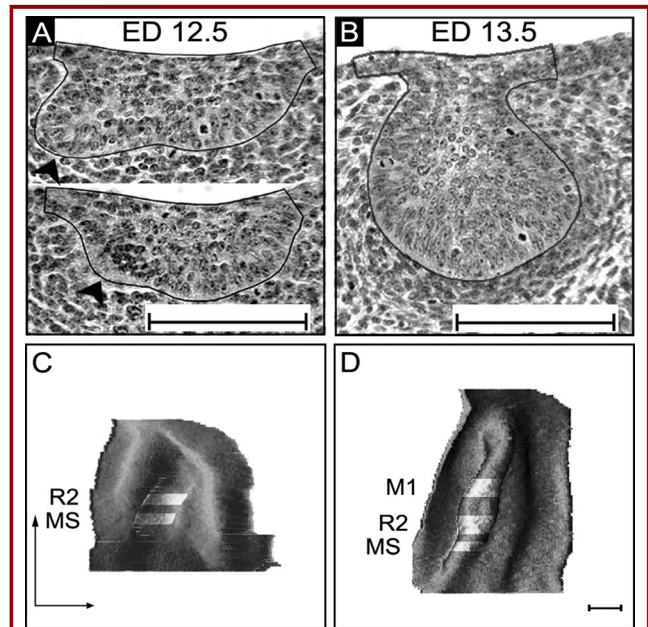


Figure 1. Rudimentary tooth primordia on sections and 3D reconstructions at ED12.5 and 13.5. (A,B) Histological sections. (A) Characteristic shape of MS (top) with lingual accessory bud (black arrowhead), its posterior disappearing (bottom) was considered as the end of the MS. (B) A wide bud morphology characteristic of the middle of the R2 region. (C,D) 3D reconstructions of dental and adjacent oral epithelium. The sections where the dental epithelium was evaluated are visualized in light strip. (C) Five sections of the MS region and five sections of the R2 region were separated by a five section (35 µm) gap at ED12.5. (D) Five sections of MS and ten sections of R2 were separated by a five section (35 µm) gap, and ten sections of M1 were separated by a ten section (70 µm) gap from the R2 at ED13.5. Scale bars: 100 µm. Vertical and horizontal arrows—posterior/lateral direction respectively.

Mitotic cells, from early metaphase to early telophase (Elalfy and Leblond, '87), were determined on photos and mitosis stage checked (at the magnification of 500×) by Leica DMLB microscope (Leica Microsystems GmbH). Mitotic index was calculated as percentage of the cells in mitosis from the total amount of cells in a cumulative sample comprising all evaluated sections in a representative region of a specific tooth primordium in all mandible halves in a group. Apoptotic elements, that is, apoptotic cells and bodies, were detected on histological sections according to morphological criteria (Tureckova et al., '96) at the magnification of 500×, using Leica DMLB microscope (Leica Microsystems GmbH). The apoptotic rate was calculated as cumulative sample of apoptotic elements related to cumulative area of dental epithelium (see mitotic index).

Whole Mount In Situ Hybridization

Embryonic mandibles were fixed in 4% PFA solution overnight at 4°C, and whole mount in situ hybridization (WISH) was carried out according to a standard protocol. DIG RNA probe was transcribed in vitro (Echelard et al., '93) from *Shh* plasmid (a kind gift from Prof. A. McMahon).

The samples were documented by a Leica MZ6 stereomicroscope with a Leica DC480 digital camera (Leica Microsystems GmbH).

Postnatal Morphometry

Our total sample comprised 258 specimens: 70 WT (32 males, 38 females), 22 *Spry2*^{-/-} (15 males, 7 females), and 166 *Spry4*^{-/-} (106 males, 42 females, and 18 with unknown sex) adult mice. A low number of jaws with a supernumerary tooth (five supernumerary teeth in *Spry2*^{-/-} and three supernumerary teeth in *Spry4*^{-/-} mice) did not allow for a statistical evaluation, and therefore only specimens without supernumerary teeth were used in the postnatal study. This approach was based on our preliminary data documenting the high frequency of the supernumerary tooth germs that start to develop and presumably can influence the M1 development, although the majority of them regress at later prenatal stages.

A dial caliper (accuracy 0.25 mm) was used to measure condylobasal length of the skull. Dental measurements focused on total antero-posterior length of the whole molar tooth row and the antero-posterior lengths of the first lower molar (M1) and its parts. The inner lobe between L1 and L2 and the tooth base between trigonid and talonid served as borders for inner measurements. To obtain dental measurements, magnifier equipped with an ocular micrometer was used with accuracy 0.05 mm for (a) and (b) and 0.025 mm for (c). From these three measurements, three other were computed: (d) length of the anteroconid region of M1 ($=a - b$), (e) length of the trigonid region of M1 ($=b - c$), and (f) length of the anteroconid-trigonid region ($=a - c$) (Fig. 2).

The degree of complexity of the anteroconid-trigonid region of M1 was determined and ranked in three phenotypic categories (Fig. 7A): standard complexity with four cusps and without any reduction in anteroconid (CO); increased complexity with a supernumerary cusp/conulid (C+); decreased complexity characterized by a reduction and drawing away of the L1 cusp, or by reduced L1/B1 cusp(s) up to remaining single, central anterior cusp (C-) (Fig. 7A).

Statistical Methods Used in Postnatal and Prenatal Morphometry

All statistics were computed using R 2.13 (CRAN, freeware) with packages "MASS" and "nlme." Analysis of independent contrasts was used to obtain basic statistical criteria ("summary" function). Log- or square-root transformation of the data was used if needed. If sex dimorphism was found, sex was used as a covariate. Statistica 10 (StatSoft, Inc., 2010) was used for graphs.

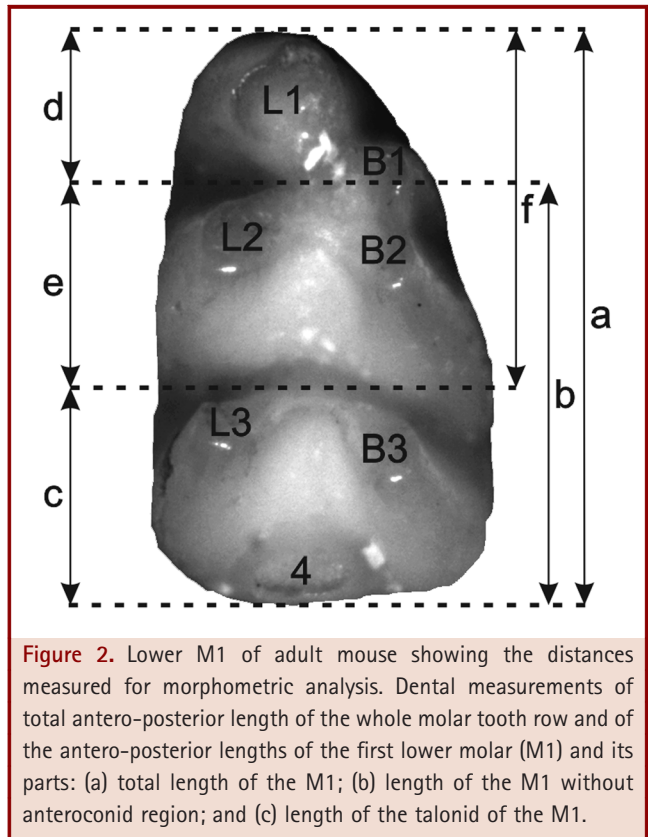


Figure 2. Lower M1 of adult mouse showing the distances measured for morphometric analysis. Dental measurements of total antero-posterior length of the whole molar tooth row and of the antero-posterior lengths of the first lower molar (M1) and its parts: (a) total length of the M1; (b) length of the M1 without anteroconid region; and (c) length of the talonid of the M1.

Analysis of variance, ANOVA (completed by subsequent Tukey test) was used for condylobasal length. Generalized linear mixed models (GLMM) with nested design (independent variable nested in jaw quadrant and it nested in specimen), specimen as a random effect and Gaussian distribution were used for dental characters. For the length of anteroconid-trigonid complex the main GLMM test was supplemented with other GLMM tests looking for differences in CO-group and among *Spry2*^{-/-} and *Spry4*^{-/-} mutants. The distribution of trigonid-anteroconid complexity in the three lineages was tested afterwards with the help of generalized linear model (GLM) with Poisson distribution.

Differences between mutants and WT mice in prenatal morphometry were tested in a similar way with one exception: Only simple ANOVA was used as the embryos' sex was not known and because our previous study did not show any significant differences between right and left side of the mandible (Kristenova et al., 2002).

RESULTS

Tooth Morphogenesis

As a first step, we compared the morphogenesis of both rudimentary tooth primordia (MS and R2) in the *Spry2*^{-/-} and

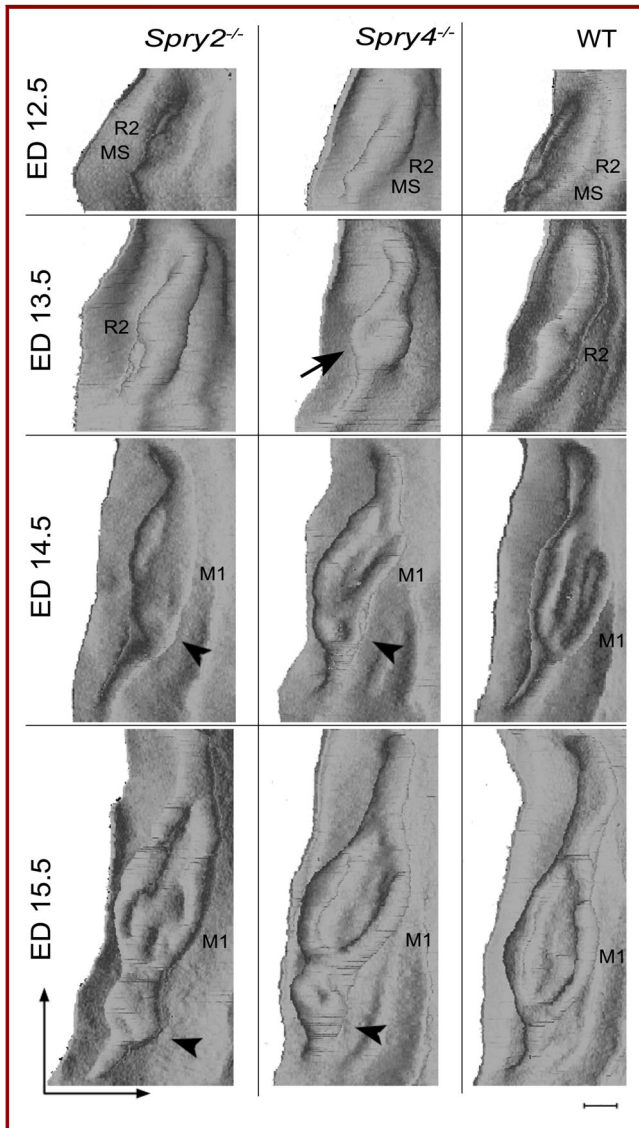


Figure 3. Plate of 3D reconstructions of dental epithelium in *Spry2*^{-/-}, *Spry4*^{-/-}, and WT at different stages. Black arrowhead shows early cap, black arrow show developing supernumerary tooth. M1—developing cap-bell of the first molar. Scale bars: 100 μm. Vertical and horizontal arrows—posterior/lateral direction respectively.

Spry4^{-/-} embryos and in WT embryos on histological sections and 3D reconstructions.

At ED12.5 in the WT embryo, two buds (MS and R2) were visible as swellings on the mound of the dental epithelium in the cheek region of mandible. The MS exhibited a typical accessory bud protruding lingually (Fig. 3). At ED13.5, the R2 bud became bigger and better differentiated, while MS development ceased because of

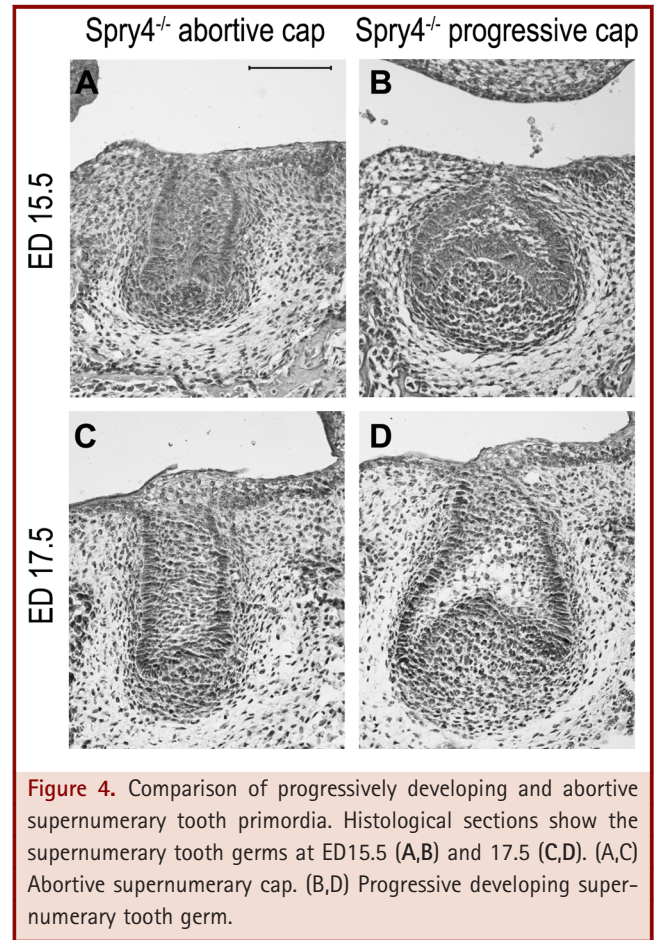


Figure 4. Comparison of progressively developing and abortive supernumerary tooth primordia. Histological sections show the supernumerary tooth germs at ED15.5 (A,B) and 17.5 (C,D). (A,C) Abortive supernumerary cap. (B,D) Progressive developing supernumerary tooth germ.

increased apoptosis in the epithelium. On 3D reconstructions and histological sections, the lingual accessory bud of the MS ceased to be visible, but the R2 bud grew into a prominent swelling and was posteriorly followed by a more narrow and long mound of molar dental epithelium. At ED14.5, the R2 bud merged with the anterior part of the developing cap of M1. At ED15.5, a well-formed M1 exhibited a cap-to-bell shaped enamel organ, and M2 started to be distinct posteriorly (Fig. 3).

At ED12.5, the dental epithelium looked similar in *Spry4*^{-/-} and WT embryos, except that the MS rudiment was more prominent in mutant embryos (Fig. 3). Interestingly, instead of the prominent R2 bud, which was present in WT embryos at ED13.5, there was already a small round cap with the appearance of histodifferentiation and enamel knot formation in all *Spry4*^{-/-} specimens. The MS was not detectable morphologically. At ED14.5, two separate caps were visible: the anterior, supernumerary cap was small and round, while the posterior M1 cap was elliptical and open-ended posteriorly, similar to the M1 cap of WT mice. Enamel knots were present in caps of both the supernumerary tooth and M1. At ED15.5, the M1 cap transformed into the bell-shaped

enamel organ. The small supernumerary cap was only observed in 75% of specimens. A narrow ridge of dental epithelium interconnecting the supernumerary cap and M1 was well visible on histological sections and 3D reconstructions (Fig. 3).

In *Spry2*^{-/-} embryos at ED12.5, the MS and R2 were identified as large swellings on the mound of dental epithelium. At ED13.5, the R2 enlarged and became a dominant structure within the cheek region. A distinct enamel knot structure (Lesot et al., '96) was present at the tip of the R2 bud (Fig. 3). The MS was still apparent anteriorly to the R2. At ED14.5, the R2 remained prominent as a large bud with its enamel knot visible on frontal sections. The M1 cap forming posteriorly from the R2 was retarded in development in comparison with WT and also *Spry4*^{-/-} specimens. However, the enamel knot in M1 was already visible. At ED15.5, R2 developed into a shallow cap that was beginning to undergo histodifferentiation and was connected by a wide epithelial strip to the M1 developing posteriorly. Histological sections confirmed that the M1 was still less differentiated (exhibiting an earlier cap stage) than in WT embryos (cap-bell transition stage). The enamel knots were morphologically detected in both caps.

In conclusion, the difference between genotypes was apparent in the timing of supernumerary tooth detection. The first sign of a marked morphological abnormality appeared at ED13.5 in *Spry4*^{-/-} samples, where a small rounded tooth cap developed, while bud-shaped epithelium was only distinct in WT and *Spry2*^{-/-} embryos (Fig. 3). The abnormal overgrowth of dental epithelium adjacent anteriorly to M1 in *Spry2*^{-/-} mice started to be clearly distinct only at ED14.5, and the supernumerary cap with a small papilla was formed at ED15.5 (Fig. 3).

Decrease in Frequency of the Supernumerary Tooth During Prenatal Development

Next, the frequency of supernumerary tooth formation was determined in mutants. A supernumerary tooth could be detected with certainty, provided that both the supernumerary tooth and the M1 exhibited a cap stage (presence of papilla regardless the level of histodifferentiation) or bell stage. Based on this criterion, the number of supernumerary caps decreased progressively during later prenatal stages. We detected the early cap in all (100%) mandibles of *Spry4*^{-/-} embryos at ED13.5. but the supernumerary cap could only be recognized with certainty in 70% of lower jaw quadrants at ED14.5. At ED18.5, the supernumerary tooth was only visible in 13% of *Spry4*^{-/-} specimens. Similarly, supernumerary tooth formation was identified in 100% of the *Spry2*^{-/-} specimens at ED15.5, but only in 42% of mandibles at ED18.5.

These data imply that the supernumerary tooth starts to develop in all mutant mice prenatally. However, in some of the mutant lower jaw quadrants, the growth and differentiation of the supernumerary tooth was arrested (Fig. 4). In the remaining mutant specimens, the supernumerary cap became larger, and its epithelium was clearly differentiated into stellate reticulum and inner and outer dental epithelium.

Morphometric Analysis of Dental Epithelium on Sections

To determine which primordia undergo revitalization, we evaluated and compared the size and apoptotic and proliferative activities in the MS and R2 epithelium at ED12.5 and ED13.5 (Fig. 1); M1 was also examined at ED13.5 (Fig. 5).

Spry2^{-/-} embryos showed lower apoptosis at ED12.5, which resulted in larger size of the dental epithelium of MS at ED13.5 compared to WT embryos. In contrast, the R2 had a smaller dental epithelium exhibiting a developmental delay in *Spry2*^{-/-} embryos at ED12.5. In *Spry2*^{-/-} samples, the growth of the R2 started at ED12.5, when proliferation was significantly higher, resulting in catch up at ED13.5. In addition, continuation of higher proliferation and decreased apoptosis in *Spry2*^{-/-} mutants at ED13.5 compared to WT mice resulted in revitalization of the R2 bud. The R2, instead of being incorporated into M1, as in WT mice, remained distinct at ED14.5 (Fig. 3). In comparison with WT samples, significantly lower apoptosis was also visible in the M1 region at ED13.5, which was followed by its slight delay in development.

In contrast to the *Spry2* mutants, the increased growth of MS rudiment in *Spry4*^{-/-} mandibles started before ED12.5, because it had reached a significantly larger size at ED12.5 compared to WT mice. Despite the absence of significant differences in apoptosis or proliferation in the MS and R2 in comparison with WT rudiments at ED12.5, the size of the epithelium of R2 was larger at ED13.5 compared to WT. This seeming paradox could be explained by a fusion of the oversized MS with the R2 rudiment, since the border between MS and R2 was not possible to determine at ED13.5. A small cap was apparent at the place of MS and R2 (Fig. 3). At ED13.5, there was a significant increase of apoptosis in the R2 and M1 region in *Spry4*^{-/-} in comparison with WT. We also noticed a significantly smaller size of the M1 region in *Spry4*^{-/-} mutants compared to WT, which was probably caused by a delay in development (Table 1).

In conclusion, the lower apoptosis and/or higher proliferation in mutants compared with WT mice resulted in the increased growth (revitalization) sequentially in the MS and R2 rudiments in *Spry2*^{-/-} mice at ED12.5 and 13.5, respectively. The process of overgrowth of the MS rudiment, its fusion with the R2 rudiment, and subsequent development seemed to begin before ED12.5.

Whole Mount In Situ *Shh* Hybridization

In order to compare the temporal-spatial dynamics of the signaling centers of the rudimentary (MS, R2) and M1 tooth primordia in Sprouty mutant versus WT embryonic mandibles, *Shh* expression was detected by whole mount in situ hybridization (Fig. 6).

Embryos harvested at a specific time naturally exhibit a range of different body weights; increasing body weight correlates with progressing tooth development. Embryos of the same chronological age were ranked in a series according to their increasing body weight, and the developmentally least and most advanced

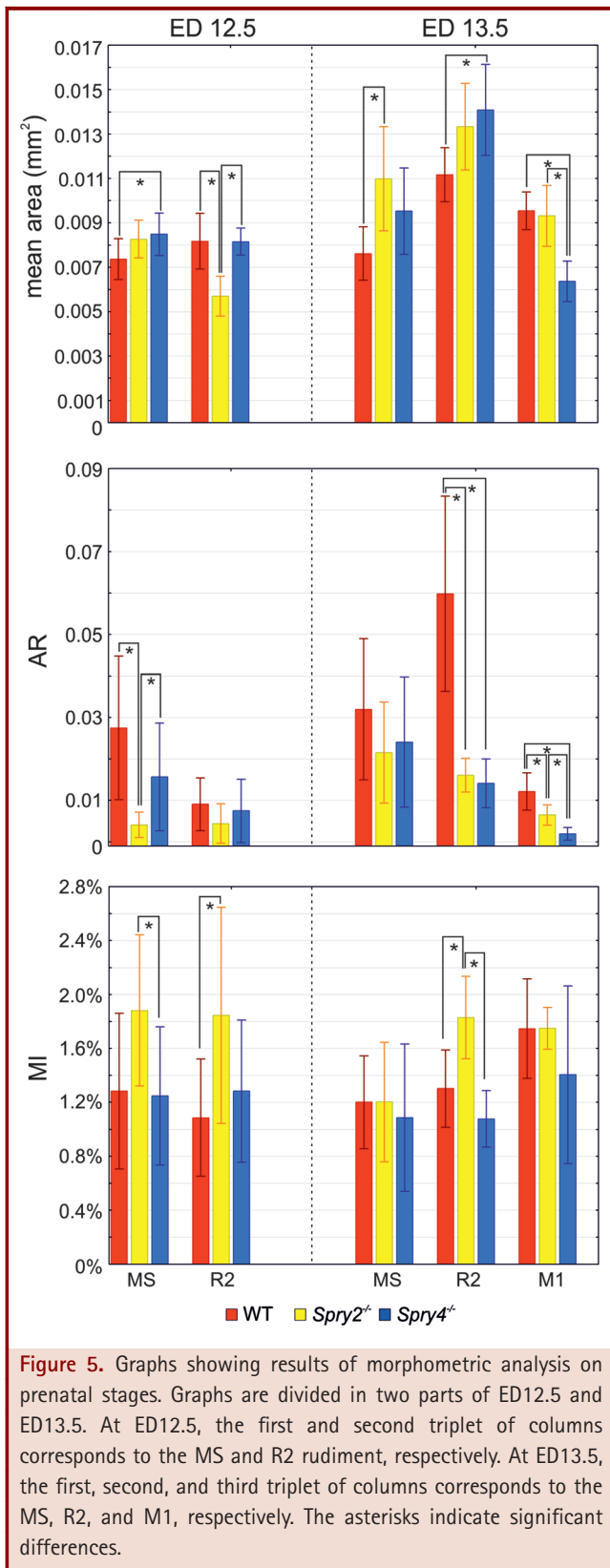


Table 1. Significant differences between Spry mutants and WT mice and P-value.

	Spry2 ^{-/-}			Spry4 ^{-/-}		
	ED12.5	ED13.5		ED12.5	ED13.5	
Area	MS	R2	M1	MS	R2	M1
Apoptotic rate	Smaller $P < 0.001$	Larger $P < 0.001$	Lower $P = 0.0015$	Larger $P = 0.0251$	Larger $P = 0.0033$	Smaller $P = 0.0251$
Mitotic index	Higher $P = 0.0257$	Lower $P < 0.001$	Higher $P < 0.001$	Lower $P < 0.001$	Lower $P < 0.001$	Lower $P < 0.001$

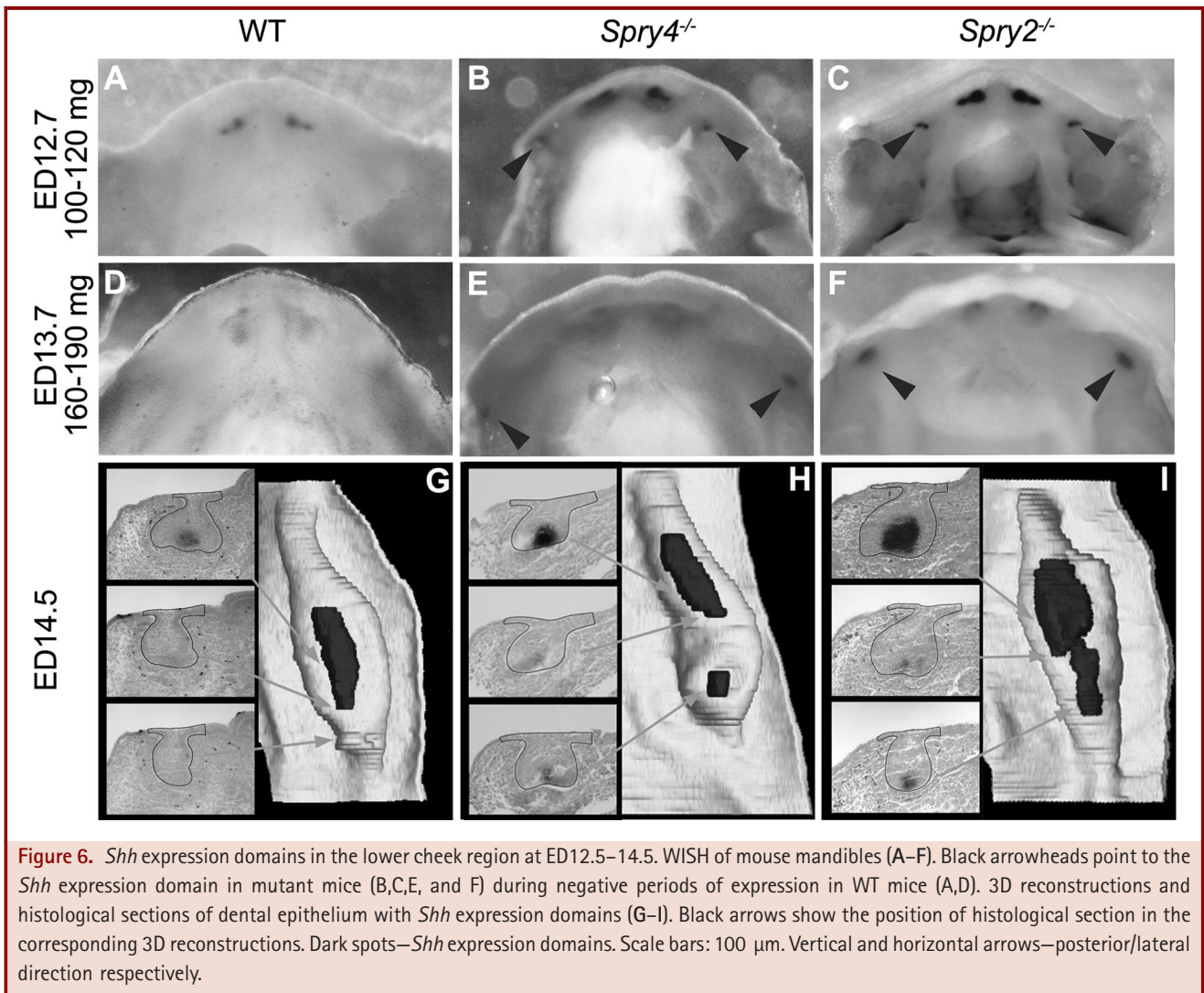


Figure 6. *Shh* expression domains in the lower cheek region at ED12.5–14.5. WISH of mouse mandibles (A–F). Black arrowheads point to the *Shh* expression domain in mutant mice (B,C,E, and F) during negative periods of expression in WT mice (A,D). 3D reconstructions and histological sections of dental epithelium with *Shh* expression domains (G–I). Black arrows show the position of histological section in the corresponding 3D reconstructions. Dark spots—*Shh* expression domains. Scale bars: 100 μ m. Vertical and horizontal arrows—posterior/lateral direction respectively.

embryos exhibited the lowest and highest body weights, respectively (Peterka et al., 2002). In such a series of WT mouse embryos from ED12, 13, or 14, one specific weight/developmental interval exists where the embryos exhibit a single spot of *Shh* expression posteriorly in the mandible. The lower and higher weight/developmental intervals, where the *Shh* spot is not present, are considered as *Shh* negative. This means that there are three positive *Shh* intervals corresponding to MS, R2, and M1 that successively appear at ED12, 13, and 14, respectively (Prochazka et al., 2010).

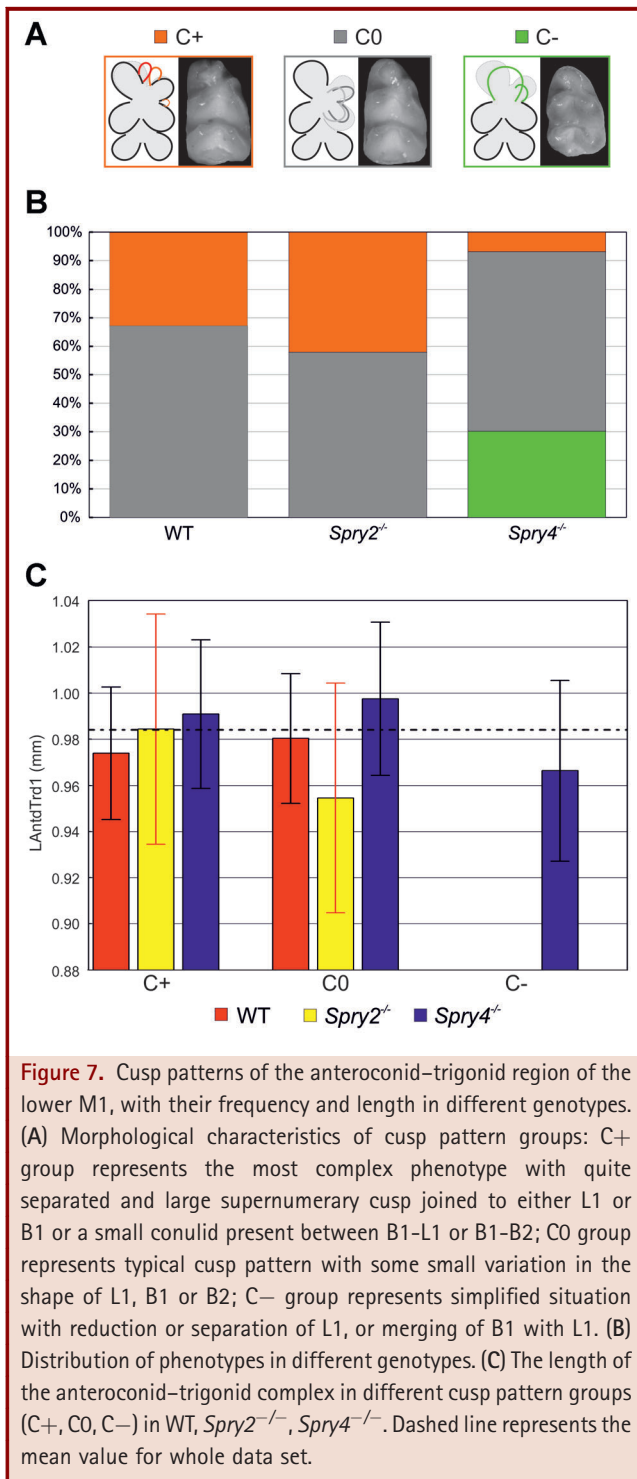
We used a similar method in this study and found that *Shh* expression of the MS, R2, and M1 successively appeared at corresponding stages also in mutant embryos, that is, during the *Shh* positive intervals in WT mice. However, the *Shh* expression domain in *Spry4*^{-/-} embryos was also detected during the

intervals that were *Shh* negative in WT mice. In the *Spry2*^{-/-} embryos, there was prolonged *Shh* expression in the MS or R2 bud, that is, the expression was present in the weight interval that was already negative in WT mice (Fig. 6A or B, respectively). In addition, *Shh* remained expressed in the R2 bud even when a typical expression domain started to be detected in the M1. This resulted in two simultaneous domains of *Shh* expression at ED14.5 (Fig. 6H,I).

In conclusion, the prolonged *Shh* expression was detected in MS and R2 rudiments in both *Spry2* and *Spry4* mutant mice compared to WT mice.

Adult Dentition

Postnatally, a supernumerary tooth was only present in 27% of lower jaw quadrants in *Spry2*^{-/-} mice and in only 2% in *Spry4*^{-/-}



mice. However, despite the low postnatal frequency of functional supernumerary teeth, the above prenatal data documented that the supernumerary tooth starts to develop in front of M1 in 100% of jaw quadrants, and thus we conclude that the majority of the

supernumerary tooth germs arrested at later prenatal stages. Since we were interested in an impact of the developing supernumerary tooth on the size and morphology of functional M1 in mutant mice, even the postnatal jaws without a functional supernumerary tooth could be used in this study.

Importantly, a significant difference was found in the distribution of cusps of the anteroconid–trigonid part of M1 ($P < 0.001$) even in the specimens without a supernumerary tooth. The *Spry4*^{-/-} mutants tended to simplified cusp pattern (C-) in the anteroconid–trigonid part of M1 (30.2% of all samples), in contrast to WT and *Spry2*^{-/-} mice, where no decreased complexity was found. Instead, the M1 in WT and *Spry2*^{-/-} mice exhibited the standard cusp pattern (Gaunt, '55; Grunberg, '65; Cermakova et al., '98) of the M1 in WT mice (C0) or a more complex anterior portion (C+): 32.9% in WT and 42.1% in *Spry2*^{-/-}. On the other hand, the C+ cusp pattern was only rarely observed in *Spry4*^{-/-} mutants (6.9%) (Fig. 7A,B).

The morphometric analysis among the complexity groups showed the following results. The anteroconid–trigonid part was significantly longer in *Spry4*^{-/-} mice ($P = 0.041$) and significantly shorter in *Spry2*^{-/-} mice ($P = 0.023$) than in WT animals exhibiting the standard cusp pattern (C0). In contrast, the *Spry4*^{-/-} molars with simplified (C-) cusp pattern had significantly shorter anteroconid–trigonid ($P < 0.001$) than those with the standard (C0) pattern.

In addition, Sprouty mutant mice had significantly increased condylobasal length (*Spry2*^{-/-} $P = 0.016$, *Spry4*^{-/-} $P < 0.001$) than WT mice, and their molar tooth row was significantly shorter (*Spry2*^{-/-} $P > 0.001$, *Spry4*^{-/-} $P > 0.001$) in the antero-posterior direction. Mutant mice had significantly shorter M1 (*Spry2*^{-/-} $P = 0.001$, *Spry4*^{-/-} $P < 0.001$), which was caused by a shorter talonid (*Spry2*^{-/-} $P = 0.004$, *Spry4*^{-/-} $P < 0.001$).

Thus, the developing supernumerary tooth has prenatal impact mainly on complexity and size of M1 in *Spry4*^{-/-} mice. There was reduced cusp number in M1 and significantly shorter anteroconid length in the abnormal M1 in *Spry4* mutant mice.

DISCUSSION

In the present study, we built on our previous examination of the revitalization of the R2 rudiment in *Spry2*^{-/-} embryos at ED13.5 (Peterkova et al., 2009) by focusing on the morphogenesis of both premolar rudimentary tooth primordia (MS, R2) in *Spry2*^{-/-} and *Spry4*^{-/-} at two time points, ED13.5 and 12.5. The dynamics of *Shh* expression was further investigated in the cheek region of the mandible (MS, R2, M1 location) in both *Spry2*^{-/-} and *Spry4*^{-/-} embryos and compared with WT embryos. Finally, the fate of the supernumerary tooth at the cap stage was described in mutants and the prenatal development correlated with adult dentition. Together, the present data suggest that the revitalization of both rudiments was involved in early development of the supernumerary tooth in Sprouty mutant mice.

Prenatal Study

During mouse odontogenesis, two large rudimentary buds progressively appear in the cheek region, and their autonomous development is subsequently suppressed by the time the first molar cap develops. These rudiments are morphologically detectable from ED12.5 (Lesot et al., '96; Peterkova et al., '96, 2000, 2002, 2003, 2006; Viriot et al., 2000). The present data document that in Sprouty mutant embryos, both rudimentary buds MS and R2 are revitalized: they were larger than in WT embryos at early stages. In addition to their size and morphology, the basic morphogenetic processes of proliferation and apoptosis were also modified in mutants. The spatial distribution of mitotic cells has been documented using 3D reconstructions during mouse M1 (Jernvall et al., '94; Lesot et al., '96; Shigemura et al., '99) and incisor (Kieffer et al., '99; Miard et al., '99) development. The quantitative evaluation of proliferation has been made in developing teeth of WT mice *in vivo* at various prenatal stages (Osman and Ruch, '75; Nso et al., '92; Lesot et al., '99), and during tooth development *in vitro* (Ahmad and Ruch, '87).

Apoptosis plays a key role in physiological suppression of the rudimentary buds and in making the toothless gap called the diastema in mice (Peterkova et al., 2003). In WT embryos, cell death is specifically concentrated in the posterior part of the upper and lower diastema, where the large premolar buds regress (Peterkova et al., '95, '96, '98; Lesot et al., '96; Viriot et al., 2000). Specific concentration of apoptosis also occurs in the enamel knot of molars (Lesot et al., '96; Vaahtokari et al., '96b; Matalova et al., 2004; Matalova et al., 2012) and in the anterior portion of M1 epithelium from ED14.5 (Lesot et al., '96; Viriot et al., 2000).

Mitotic cells are distributed throughout the dental epithelium in the lower cheek region at ED12.5 (Viriot et al., '97). At ED13.5, cell divisions stop in two discrete (BrdU negative) areas located in the most anterior part of the developing dental epithelium and in the prospective primary enamel knot (Shigemura et al., '99). In accordance with the present data, the two BrdU negative areas located in the most anterior part of the developing dental epithelium at ED13.5 observed by Shigemura et al., '99 can be reinterpreted as corresponding to the MS and R2, respectively. Indeed, lower mitotic indexes were found in WT mice in the MS and R2 regions in comparison with M1 region. However, in *Spry2*^{-/-} mice, the MS or R2 rudiments exhibited similar mitotic indexes as the M1. In contrast, apoptosis, which normally accumulates in the MS at ED12.5 and in both the MS and R2 at ED13.5, was not observed in *Spry2*^{-/-} embryos, except for the MS region at ED13.5 (Fig. 5). This is concordant with the proposed role of the SPRY2 as a regulator of apoptosis: the silencing of the human *Spry2* has been connected with anti-apoptotic action in serum (Edwin and Patel, 2008).

We expected the levels of mitosis and apoptosis in *Spry4*^{-/-} embryos to be similar to the *Spry2*^{-/-} embryos. Interestingly, the mitotic indexes in MS (ED12.5) and R2 (ED13.5) were not significantly lower in *Spry4*^{-/-} than in WT embryos, but they

were significantly lower than in *Spry2*^{-/-} embryos. These differences between *Spry2*^{-/-} and *Spry4*^{-/-} specimens suggest that the changes in cellular process leading to the increased size of *Spry4*^{-/-} dental epithelium in the MS already at ED12.5 had to start before ED12.5. However, significantly less apoptosis was found in the R2 and M1 region of *Spry4*^{-/-} embryos at ED13.5, when compared with WT (Fig. 5). The lack of apoptosis in the R2 region helped the MS/R2 cap to give rise to a supernumerary tooth and in the delayed M1 to catch up in *Spry4*^{-/-} embryos.

Shh Expression

Besides the expected *Shh* expression in the signaling center (primary enamel knot) in the M1 at ED14.5 (Jernvall et al., '94; Iseki et al., '96; Koyama et al., '96), the existence of other signaling centers also expressing *Shh* has been recently experimentally demonstrated in rudimentary tooth primordia in mice: in the cheek teeth region at ED12.5 and 13.5 (Prochazka et al., 2010) and the incisor region at the same stages (Hovorakova et al., 2011). *Shh* expression has been also found in the rudimentary dental epithelium in the upper diastema of the mouse and vole (Keranen et al., '99).

We found a series of *Shh* expression domains that appeared sequentially in MS, R2, and M1 being separated by *Shh* negative intervals, as described in WT mice (Prochazka et al., 2010). Interestingly, *Shh* was also expressed in the rudiments in both *Spry2*^{-/-} and *Spry4*^{-/-} embryos in the developmental intervals, which were *Shh* negative in WT mice (Fig. 6). *Shh* expression may be indirectly influenced by Sprouty genes, and it has previously been suggested that *Shh* is upregulated by Fgfs (Klein et al., 2006).

Shh plays a key role during morphogenesis of a tooth primordium (Dassule et al., 2000). Interestingly, either loss of *Shh* function (Cobourne et al., 2001; Ohazama et al., 2009) or the abundance of *Shh* function result in decreases in cell proliferation, and tooth development is arrested at the bud stage (Cobourne et al., 2009). Therefore, the appropriate regulating of *Shh* signaling is important for cell homeostasis during tooth development (Cobourne et al., 2009). In addition *Shh* seems to inhibit cusp patterning (Harjunmaa et al., 2012).

It appears that *Shh* normally participates in arresting the growth of the central part of the tooth germ (the area of the enamel knot), and also that *Fgf* signaling induces the growth of the lateral parts of the dental epithelium (Jernvall et al., '94, '98; Vaahtokari et al., '96a). We thus hypothesize that the ectopic *Shh* expression in *Spry4* mutants and consequent upregulation of *Fgf* family members in rudimentary buds might stimulate a bud-cap transition in the developing supernumerary tooth at ED13.5. The Sprouty genes may also regulate an interaction between Fgf and the Wnt pathway. Interestingly, upregulation of the Wnt pathway led to the revitalization of the R2 bud, and this effect was counteracted by *Shh* (Ahn et al., 2010).

A question may arise about the timing of the effects of different Sprouty genes. The present data suggest that the absence of *Spry4*

supports the revitalization of the rudiments earlier than the absence of *Spry2*, resulting in a larger size of the dental epithelium at ED12.5 and supernumerary cap origin at ED13.5 in *Spry4*^{-/-} embryos (Fig. 5). However, the absence of *Spry4* seems to only minimally support the later development (after ED13.5) of the supernumerary tooth, since this structure becomes progressively suppressed in most *Spry4* mutant fetuses (Fig. 4). In contrast, the absence of *Spry2* seems to support the supernumerary tooth formation from a later stage, but its positive effect acts for a longer period. This might explain why only 2% of *Spry4*^{-/-} adult mice had supernumerary teeth in contrast to 27% of *Spry2*^{-/-} animals in this study. It is known that *Spry2* is expressed in the epithelium while *Spry4* in the mesenchyme (Klein et al., 2006). We propose that this difference in the compartmental expression of Sprouty genes is related to the differences in revitalization of the rudimentary tooth primordia and in the survival of the supernumerary tooth germ, as occurs in *Spry2*^{-/-} and *Spry4*^{-/-} mutants.

Evolutionary-Developmental Implications

A progressive reduction of premolars can be traced through the evolutionary changes that occurred from early rodents to modern Muridae (Fig. 8). Members of the stem lineage of Rodentia from the early Tertiary, Eurymylidae, still possessed two or three premolars and a very simple M1 without the anteroconid (Meng et al., 2003, 2005). Later in the evolution of rodents, there was only one premolar present until the splitting of Myomorpha, where all lower premolars are suppressed. Although several teeth were suppressed and lost from the adult dentition, two large rudimentary tooth primordia still transiently develop in the posterior diastema in

mouse embryos, which have been related to the lost premolars (Peterkova et al., '96, 2000, 2002; Viriot et al., 2002). In the mouse mandible, it has been experimentally demonstrated that the posterior premolar rudiment R2 finally becomes incorporated into the anterior portion of the M1 cap (Prochazka et al., 2010), and the anterior premolar rudiment MS take place in the anterior slope of the M1 enamel organ (Ahn et al., 2010). These data confirm the classical hypothesis that the material from lost premolars in rodents could participate in the formation of the anterior region of M1 that was first suggested more than 100 years ago (Adloff, 1898), and which has been later supported by morphological (Peterkova, '83; Peterkova et al., 2002, 2005) and paleontological (Viriot et al., 2002) data.

The impact of the supernumerary tooth formation on the size/shape of M1 has previously been explored (Gruneberg, '65; Sofaer, '69; Kristenova et al., 2002; Tucker et al., 2004). Posteriorly to the supernumerary tooth, a shortening in the anterior part of the M1 without major cusp changes was found in *Spry2*^{-/-} mice (Klein et al., 2006); *Lrp4*^{-/-} and Wise mice exhibit fusion of M1 and M2 (Ohazama et al., 2008; Haara et al., 2012). Better-differentiated anterior cusps and medial cusp crests were observed in the M1 in K14-Eda mice (Kangas et al., 2004), and buccal cusp crests have been reported in *Ectodin*^{-/-} mice (Kassai et al., 2005; Ahn et al., 2010).

Supernumerary teeth also exist in the *Spry2*^{-/-} and *Spry4*^{-/-} mice (Klein et al., 2006). Their lower frequency in the *Spry2*^{-/-} and *Spry4*^{-/-} mice used for this study contrasts with our previous report (Klein et al., 2006) and is likely attributable to shifts in genetic background over time. However, a potential for formation of the supernumerary tooth was clearly apparent during early stages (Fig. 3) in 100% of embryos/fetuses of Sprouty mutants. Thus, we could find changes in the adult Sprouty mutant dentition, even though the functional supernumerary tooth was not present. The M1 as well as the whole molar block were significantly shorter in both *Spry2*^{-/-} and *Spry4*^{-/-} mice compared to WT mice. But, surprisingly, only the anteroconid-trigonid complex of M1 was relatively enlarged, being about equal in length compared to that of WT mice. In addition, there were significant changes of cusp pattern complexity in *Spry2*^{-/-} and *Spry4*^{-/-} mice, which tended to increase and decrease, respectively, in comparison with WT mice (Fig. 7). However, the cusp complexity changes (supernumerary cusp) were found in almost 30% specimens of WT mice. These changes reflected the fact that anteroconid-trigonid complex is evolutionary unstable, as has been described recently (Boran et al., 2005).

Variations in the degree of the incorporation of the rudimentary anlage of the premolar dentition might be responsible for shape variability in the anterior part of upper M1 in the laboratory mouse (Peterkova, '83, Peterkova et al., '95, 2006), as well as in the house mouse from Corsica (Renaud et al., 2011). In some mutant mice, the premolar rudiment follows its autonomous development, leading to the formation of a supernumerary tooth, instead of being

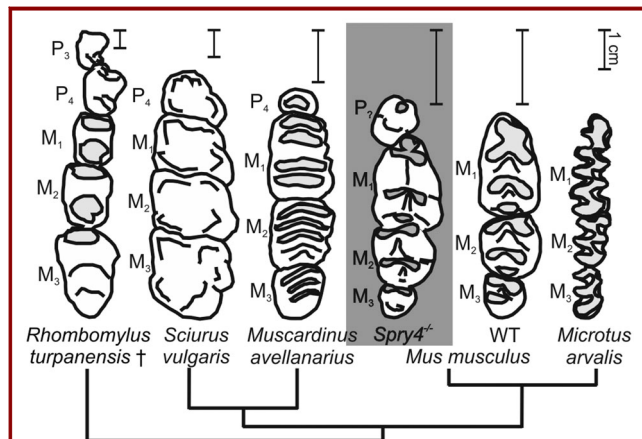


Figure 8. Evo-devo aspects and hypothesis. A scheme of disappearance of premolars during evolution of Muroids. By the presence of a tooth in front of M1, the Sprouty mice (in gray) are reminiscent to evolutionary ancestors of Muroids with preserved premolar tooth.

incorporated into the M1 anlage. Failure in the incorporation of the rudiment results in a reduction of the anterior part of M1 (Peterkova, '83; Peterkova et al., 2002). The reduction of the anterior (anteroconid) part of the M1, as observed in heterozygous Tabby/Eda mice, has been explained in a similar way (Peterkova et al., 2005). Thus, the changes observed in the anterior part of the adult M1 (Fig. 7) might be explained by differential effects of the incorporation (participation) of the premolar rudiments on M1 development. In *Spry4*^{-/-} embryos, the size of the MS bud was already enlarged at ED12.5, suggesting growth stimulation before this time point. Later on, mitosis and apoptosis in both rudiments remained at the level similar to WT mice (except for the decreased apoptosis in the R2 region at ED13.5). Therefore, we propose that the MS rudiment participates more heavily in supernumerary tooth development in *Spry4* than in *Spry2* mutants. Regardless, the supernumerary tooth was aborted prenatally; its development impacted the formation of the anterior part of M1. The reduction of the size and/or complexity of M1 might result from involvement of the rudimentary tissues in the supernumerary tooth development instead of in the development of the anterior part of M1. The elongation or increased complexity in the anterior part of the M1 might result from incomplete separation or secondary fusion between the M1 and the aborted supernumerary tooth primordium. The differences between *Spry2*^{-/-} and *Spry4*^{-/-} samples suggest different developmental interactions between the supernumerary tooth and M1. These data support the notion that rudiments, in general, can persist quite a long time in the history of species (Darwin, 1859) and can be reused for building or innovation of structures anytime later (Hall, 2003).

Although the premolars had been suppressed during evolution of Muridae, the situation is quite different in the sister group of Rodentia, Lagomorpha, where the two premolars still endure (Ungar, 2010), as in Eurymylidae. Our data suggest that reduction of premolars and consequent establishment of differences between the two mammalian orders may be associated with regulatory mutations in Sprouty genes or in other genes in the *Fgf* pathway, as previously proposed for mouse incisors (Charles et al., 2009). Accordingly, when the balance of regulatory genes is disrupted, premolars lost in evolution of Rodentia may reappear as supernumerary teeth. The present study on Sprouty mutant mice suggests that these animals are a good tool to approach questions on the regulatory mechanisms implicated during evolution of rodent dentition and can help in understanding the etiopathogenesis of supernumerary teeth.

ACKNOWLEDGMENTS

We thank A. McMahon (Harvard University, Cambridge, MA) for kindly providing the *Shh* plasmid, L. Smrckova for providing a part of material and the other staff for technical assistance. This work was supported by Grant Agency of the Czech Republic (CZ: GA ĀR:GAP305/12/1766).

LITERATURE CITED

- Adloff P. 1898. Zur entwicklungsgeschichte des nagetiergebisses/von Paul Adloff. Jena: Gustav Fischer. [in German]
- Ahmad N, Ruch JV. 1987. Comparison of growth and cell-proliferation kinetics during mouse molar odontogenesis in vivo and in vitro. *Cell Tissue Kinet* 20:319–329.
- Ahn Y, Sanderson BW, Klein OD, Krumlauf R. 2010. Inhibition of Wnt signaling by *wise* (*Sostdc1*) and negative feedback from *Shh* controls tooth number and patterning. *Development* 137:3221–3231.
- Boran T, Lesot H, Peterka M, Peterkova R. 2005. Increased apoptosis during morphogenesis of the lower cheek teeth in tabby/EDA mice. *J Dent Res* 84:228–233.
- Caton J, Tucker AS. 2009. Current knowledge of tooth development: patterning and mineralization of the murine dentition. *J Anat* 214:502–515.
- Cermakova P, Peterka M, Capkova J, et al. 1998. Comparison of the tooth shape and size in tabby and non-tabby mice. *Acta Vet Brno* 67:3–14.
- Charles C, Pantalacci S, Peterkova R, Tafforeau P, Laudet V, Viriot L. 2009. Effect of EDA loss of function on upper jugal tooth morphology. *Anat Rec* 292:299–308.
- Cobourne MT, Sharpe PT. 2010. Making up the numbers: the molecular control of mammalian dental formula. *Semin Cell Dev Biol* 21:314–324.
- Cobourne MT, Hardcastle Z, Sharpe PT. 2001. Sonic hedgehog regulates epithelial proliferation and cell survival in the developing tooth germ. *J Dent Res* 80:1974–1979.
- Cobourne MT, Xavier GM, Depew M, et al. 2009. Sonic hedgehog signalling inhibits palatogenesis and arrests tooth development in a mouse model of the nevoid basal cell carcinoma syndrome. *Dev Biol* 331:38–49.
- Darwin C. 1859. On the origin of species. A facsimile of the first edition. Cambridge, MA: Harvard University Press. Sixteenth printing, 2000.
- Dassule HR, Lewis P, Bei M, Maas R, McMahon AP. 2000. Sonic hedgehog regulates growth and morphogenesis of the tooth. *Development* 127:4775–4785.
- Echelard Y, Epstein DJ, St Jacques B, et al. 1993. Sonic hedgehog, a member of a family of putative signaling molecules, is implicated in the regulation of CNS polarity. *Cell* 75:1417–1430.
- Edwin F, Patel TB. 2008. A novel role of Sprouty 2 in regulating cellular apoptosis. *J Biol Chem* 283:3181–3190.
- Elalfy M, Leblond CP. 1987. Long duration of mitosis and consequences for the cell-cycle concept, as seen in the isthmal cells of the mouse pyloric antrum. 1. Identification of early and late steps of mitosis. *Cell Tissue Kinet* 20:205–213.
- Gaunt WA. 1955. The development of the molar pattern of the mouse (*Mus musculus*). *Acta Anat (Basel)* 24:249–268.
- Gruneberg H. 1955. Heterosis and variability in the mouse. *Proc R Soc Lond B Biol Sci* 144:220–221.
- Gruneberg H. 1965. Genes and genotypes affecting the teeth of the mouse. *J Embryol Exp Morphol* 14:137–159.

- Haara O, Harjunmaa E, Lindfors PH, et al. 2012. Ectodysplasin regulates activator-inhibitor balance in murine tooth development through Fgf20 signaling. *Development* 139:3189–3199.
- Hacohen N, Kramer S, Sutherland D, Hiromi Y, Krasnow MA. 1998. Sprouty encodes a novel antagonist of FGF signaling that patterns apical branching of the *Drosophila* airways. *Cell* 92:253–263.
- Hall BK. 2003. Descent with modification: the unity underlying homology and homoplasy as seen through an analysis of development and evolution. *Biol Rev* 78:409–433.
- Harjunmaa E, Kallonen A, Voutilainen M, Hamalainen K, Mikkola ML, Jernvall J. 2012. On the difficulty of increasing dental complexity. *Nature* 483:324–327.
- Hovorakova M, Prochazka J, Lesot H, et al. 2011. *Shh* expression in a rudimentary tooth offers new insights into development of the mouse incisor. *J Exp Zool B* 316B:347–358.
- Iseki S, Araga A, Ohuchi H, et al. 1996. Sonic hedgehog is expressed in epithelial cells during development of whisker, hair, and tooth. *Biochem Biophys Res Commun* 218:688–693.
- Jernvall J, Kettunen P, Karavanova I, Martin LB, Thesleff I. 1994. Evidence for the role of the enamel knot as a control center in mammalian tooth cusp formation: non-dividing cells express growth stimulating Fgf-4 gene. *Int J Dev Biol* 38:463–469.
- Jernvall J, Aberg T, Kettunen P, Keranen S, Thesleff I. 1998. The life history of an embryonic signaling center: Bmp-4 induces p21 and is associated with apoptosis in the mouse tooth enamel knot. *Development* 125:161–169.
- Kangas AT, Evans AR, Thesleff I, Jernvall J. 2004. Nonindependence of mammalian dental characters. *Nature* 432:211–214.
- Kassai Y, Munne P, Hotta YH, et al. 2005. Regulation of mammalian tooth cusp patterning by ectodin. *Science* 309:2067–2070.
- Keranen SVE, Kettunen P, Aberg T, Thesleff I, Jernvall J. 1999. Gene expression patterns associated with suppression of odontogenesis in mouse and vole diastema regions. *Dev Genes Evol* 209:495–506.
- Kieffer S, Peterkova R, Vonesch JL, Ruch JV, Peterka M, Lesot H. 1999. Morphogenesis of the lower incisor in the mouse from the bud to early bell stage. *Int J Dev Biol* 43:531–539.
- Klein OD, Minowada G, Peterkova R, et al. 2006. Sprouty genes control diastema tooth development via bidirectional antagonism of epithelial-mesenchymal FGF signaling. *Dev Cell* 11:181–190.
- Koyama E, Yamaai T, Iseki S, et al. 1996. Polarizing activity, sonic hedgehog, and tooth development in embryonic and postnatal mouse. *Dev Dyn* 206:59–72.
- Kristenova P, Peterka M, Lisi S, Gendault JL, Lesot H, Peterkova R. 2002. Different morphotypes of functional dentition in the lower molar region of tabby (EDA) mice. *Orthod Craniofac Res* 5:205–214.
- Lesot H, Vonesch JL, Peterka M, Tureckova J, Peterkova R, Ruch JV. 1996. Mouse molar morphogenesis revisited by three-dimensional reconstruction. 2. Spatial distribution of mitoses and apoptosis in cap to bell staged first and second upper molar teeth. *Int J Dev Biol* 40:1017–1031.
- Lesot H, Peterkova R, Schmitt R, et al. 1999. Initial features of the inner dental epithelium histo-morphogenesis in the first lower molar in mouse. *Int J Dev Biol* 43:245–254.
- Matalova E, Tucker AS, Sharpe PT. 2004. Death in the life of a tooth. *J Dent Res* 83:11–16.
- Matalova E, Svandova E, Tucker AS. 2012. Apoptotic signaling in mouse odontogenesis. *OMICS* 16:60–70.
- Meng J, Hu YM, Li CK. 2003. The osteology of rhombomylus (Mammalia, Glires): implications for phylogeny and evolution of Glires. *Bull Am Museum Nat Hist* 275:1–247.
- Meng J, Wyss AR, Hu YM, Wang YQ, Bowen GJ, Koch PL. 2005. Glires (Mammalia) from the late Paleocene Bayan Ulan locality of Inner Mongolia. *Am Museum Novitates* 3473:1–25.
- Miard S, Peterkova R, Vonesch JL, Peterka M, Ruch JV, Lesot H. 1999. Alterations in the incisor development in the tabby mouse. *Int J Dev Biol* 43:517–529.
- Neubuser A, Peters H, Balling R, Martin GR. 1997. Antagonistic interactions between FGF and BMP signaling pathways: a mechanism for positioning the sites of tooth formation. *Cell* 90:247–255.
- Nso M, Senger B, Ruch JV. 1992. Scoring mitotic activity in longitudinal sections of mouse embryonic incisors: significant differences exist for labial and lingual inner dental epithelia. *J Craniofac Genet Dev Biol* 12:159–166.
- Ohazama A, Johnson EB, Ota MS, et al. 2008. Lrp4 modulates extracellular integration of cell signaling pathways in development. *PLoS ONE* 3:1–11.
- Ohazama A, Haycraft CJ, Seppala M, et al. 2009. Primary cilia regulate *Shh* activity in the control of molar tooth number. *Development* 136:897–903.
- Osman A, Ruch JV. 1975. Topographical distribution of mitosis in odontogenic fields of lower jaw in mice embryos. *J Biol Buccale* 3:117–132.
- Peterka M, Lesot H, Peterkova R. 2002. Body weight in mouse embryos specifies staging of tooth development. *Connect Tissue Res* 43:186–190.
- Peterkova R. 1983. Dental lamina develops even within the mouse diastema. *J Craniofac Genet Dev Biol* 3:133–142.
- Peterkova R, Peterka M, Vonesch JL, Ruch JV. 1995. Contribution of 3-D computer-assisted reconstructions to the study of the initial steps of mouse odontogenesis. *Int J Dev Biol* 39:239–247.
- Peterkova R, Lesot H, Vonesch JL, Peterka M, Ruch JV. 1996. Mouse molar morphogenesis revisited by three dimensional reconstruction. 1. Analysis of initial stages of the first upper molar development revealed two transient buds. *Int J Dev Biol* 40:1009–1016.
- Peterkova R, Peterka M, Vonesch JL, et al. 1998. Correlation between apoptosis distribution and BMP-2 and BMP-4 expression in vestigial tooth primordia in mice. *Eur J Oral Sci* 106:667–670.
- Peterkova R, Peterka M, Viriot L, Lesot H. 2000. Dentition development and budding morphogenesis. *J Craniofac Genet Dev Biol* 20:158–172.
- Peterkova R, Peterka M, Viriot L, Lesot H. 2002. Development of the vestigial tooth primordia as part of mouse odontogenesis. *Connect Tissue Res* 43:120–128.

- Peterkova R, Peterka M, Lesot H. 2003. The developing mouse dentition—a new tool for apoptosis study. In: Diederich M, editor. *Apoptosis: from signaling pathways to therapeutic tools*. vol 2010. New York: N. Y. Acad. Sci. p 453–466.
- Peterkova R, Lesot H, Viriot L, Peterka M. 2005. The supernumerary cheek tooth in tabby/EDA mice—a reminiscence of the premolar in mouse ancestors. *Arch Oral Biol* 50:219–225.
- Peterkova R, Lesot H, Peterka M. 2006. Phylogenetic memory of developing mammalian dentition. *J Exp Zool B* 306B:234–250.
- Peterkova R, Churava S, Lesot H, et al. 2009. Revitalization of a diastemal tooth primordium in *Spry2* null mice results from increased proliferation and decreased apoptosis. *J Exp Zool B* 312B:292–308.
- Peters H, Balling R. 1999. Teeth—where and how to make them. *Trends Genet* 15:59–65.
- Porntaveetus T, Ohazama A, Choi HY, Herz J, Sharpe PT. 2011a. Wnt signaling in the murine diastema. *Eur J Orthod* 34:518–524.
- Porntaveetus T, Otsuka-Tanaka Y, Basson MA, Moon AM, Sharpe PT, Ohazama A. 2011b. Expression of fibroblast growth factors (FGFs) in murine tooth development. *J Anat* 218:534–543.
- Prochazka J, Pantalacci S, Churava S, et al. 2010. Patterning by heritage in mouse molar row development. *Proc Natl Acad Sci USA* 107:15497–15502.
- Renaud S, Pantalacci S, Auffray JC. 2011. Differential evolvability along lines of least resistance of upper and lower molars in island house mice. *PLoS ONE* 6:1–9.
- Shigemura N, Kiyoshima T, Kobayashi I, et al. 1999. The distribution of BrdU- and TUNEL-positive cells during odontogenesis in mouse lower first molars. *Histochem J* 31:367–377.
- Shim K, Minowada G, Coling DE, Martin GR. 2005. *Sprouty2*, a mouse deafness gene, regulates cell fate decisions in the auditory sensory epithelium by antagonizing FGF signaling. *Dev Cell* 8:553–564.
- Sofaer JA. 1969. Aspects of the tabby-crinkled-downless syndrome. I. The development of tabby teeth. *J Embryol Exp Morphol* 22:181–205.
- Tucker AS, Headon DJ, Courtney JM, Overbeek P, Sharpe PT. 2004. The activation level of the TNF family receptor, Edar, determines cusp number and tooth number during tooth development. *Dev Biol* 268:185–194.
- Tureckova J, Lesot H, Vonesch JL, Peterka M, Peterkova R, Ruch JV. 1996. Apoptosis is involved in the disappearance of the diastemal dental primordia in mouse embryo. *Int J Dev Biol* 40:483–489.
- Ungar PS. 2010. *Mammal teeth: origin, evolution, and diversity*. Baltimore, USA: Johns Hopkins University Press.
- Vahtokari A, Aberg T, Jernvall J, Keranen S, Thesleff I. 1996a. The enamel knot as a signaling center in the developing mouse tooth. *Mech Dev* 54:39–43.
- Vahtokari A, Aberg T, Thesleff I. 1996b. Apoptosis in the developing tooth: association with an embryonic signaling center and suppression by EGF and FGF-4. *Development* 122:121–129.
- Viriot L, Lesot H, Vonesch JL, Ruch JV, Peterka M, Peterkova R. 2000. The presence of rudimentary odontogenic structures in the mouse embryonic mandible requires reinterpretation of developmental control of first lower molar histomorphogenesis. *Int J Dev Biol* 44:233–240.
- Viriot L, Peterkova R, Peterka M, Lesot H. 2002. Evolutionary implications of the occurrence of two vestigial tooth germs during early odontogenesis in the mouse lower jaw. *Connect Tissue Res* 43:129–133.
- Viriot L, Peterkova R, Vonesch JL, Peterka M, Ruch JV, Lesot H. 1997. Mouse molar morphogenesis revisited by three-dimensional reconstruction. 3. Spatial distribution of mitoses and apoptoses up to bell-staged first lower molar teeth. *Int J Dev Biol* 41:679–690.
- Wang XP, Fan JB. 2011. Molecular genetics of supernumerary tooth formation. *Genesis* 49:261–277.